Behaviour of hydrodynamic journal bearing under the combined influence of textured surface and Non-Newtonian Rabinowitsch fluid model

Belkacem MANSER[1,*], *Sofiane* KHELLADI[2], *Michael* DELIGANT[2], *Haroun* RAGUEB[1], *Idir* BELAIDI[1], and *Farid* BAKIR[2]

[1]LEMI., FT., University of M'hamed Bougara, Avenue de I'indépendance, 35000-Boumerdes, Algeria.
[2]Arts et Métiers Institute of Technology, CNAM, LIFSE, HESAM University, F-75013 Paris, France.

Abstract. In the present study, the static characteristics of hydrodynamic circular journal bearings of finite length are highlighted, using the combined influences of textured surface and non-Newtonian lubricants behavior, obeying to the Rabinowitsch fluid model. The associated nonlinear Rabinowitsch-Reynolds equation has been discretized using finite differences scheme and solved by the mean of Elrod's algorithm taking into account the presence of cylindrical textures on full/optimum bearing surface. Following to the absence of textures on the bearing surface or the non-Newtonian fluid behavior, the obtained results are in good agreement with the reference ones. The hydrodynamic lubrication static performances are computed for various parameters such as textures location; eccentricity ratio and the rheological coefficient. The results suggest that texturing the bearing's convergent zone enhances significantly the load carrying capacity and reduces the friction coefficient, whereas texturing the full bearing surface may leads to bad performances. It is also noticed that the pseudoplastic lubricant coefficient decreases the bearing performances (load capacity and pressure) compared to Newtonian fluid cases. Considering the optimal arrangement of textures on the contact surface, a significant improvement in terms of load capacity and friction can be achieved, especially at low pseudoplasticity effect.

keywords. Hydrodynamic journal bearing; Surface texturing; Cavitation effect; Non-Newtonian fluid; Rabinowitsch fluid model.

1 Introduction

Fluid film journal bearings are nowadays extensively used in heavy rotating machineries. They widely employed, in adverse industrial conditions, due to their wide ranges of load-carrying ability to support heavy loads, especially at high operating parameters [1]. Typically, it has been reported that these machine components present the most important power losses and detrimental effects in rotating machines, due to the vibration, wear and misalignment at the interfaces of rotor/bearings [2]. Consequently, bearing systems must be designed to operate under different loads, speeds and environments with high performances and minimal noise and vibration. Therefore, over the past two decades, many researchers [3] have investigated

*e-mail: b.manser@univ-boumerdes.dz

the performance characteristics of the journal bearings lubricated with non-Newtonian fluids. They reported that, base oil blended with small amounts of long chain polymer are very efficient to enhance the bearing performances. While others [4] have attempted to address the precise control of surface properties on the functional operating of mechanical systems. The findings were that, the lubricating characteristics of bearing devices can be enhanced by the incorporation of specific texture shapes into the correct contact interface arrangement. Several theoretical and experimental studies have been carried out to describe the behavior of fluid additives on the performance characteristics of lubricating mechanisms, such as the micropolar model [5], couple stress model [6], power law [7] and Rabinowitsch model [8, 9]. Recently, the emphasis has been placed in Rabinowitsch fluid model [10, 11]. Many studies were conducted to analyze the effects of this fluid model on the characteristics of various lubricating contacts [12–14]. However, journal bearings with different geometrical configurations [15–17], operating conditions [18–20] and influencing factors [21–23] are the most studied sliding bearings. The achieved results indicate unfavorable bearing performances with pseudo-plastic Rabinowitsch lubricant as compared to Newtonian fluid.
The above-mentioned works was performed based on Newtonian fluids and smooth surfaces. Considering the non-Newtonian lubricant and textured bearing, Kango et al. [24] investigated the combined influences of surface texturing and non-Newtonian "power law" fluid model on the hydrodynamic lubrication of finite journal bearings. It was reported that the best performance enhancement was achieved when the surface texturing is considered in only convergent zone of the bearing. Very recently, a numerical investigation related to the combined influences of bearing surface texturing and lubricating effectiveness of "micropolar fluids", on the performances of hydrodynamic finite groove journal bearings, was conducted by Manser et al. [25]. A Cylindrical "CY" texture shape in full and optimum locations, and micropolar fluid variations were considered. It was found that the combined effects of fully surface textured with micropolar fluids causes poor performances. Nevertheless, optimal arrangement of textures on the contact surface significantly improves the bearing performances. It is worth noting here that none of these researchers have conducted an investigation into the issue of textured bearings using the Rabinowitsch fluid model. Thus, the objective of this paper is to present numerical study for exploring the influence of non-Newtonian pseudo-plastic lubricants using "Rabinowitsch" fluid model on the hydrodynamic textured journal bearing efficiency.

2 Governing equations

2.1 Modified Reynolds equation and Elrod cavitation algorithm

For an in-compressible fluid, in steady state laminar flow, under the isothermal condition, the nonlinear mass conservative form of Rabinowitsch-Reynolds equation (in Cartesian coordinates) can be expressed as follows :

$$\frac{\partial}{\partial\theta}\left\{\left[\frac{h^3}{12}\,g\beta\,\frac{\partial\Theta}{\partial\theta}+\alpha\,\frac{h^5}{80}\left(g\beta\,\frac{\partial\Theta}{\partial\theta}\right)^3\right]\right\}+\left(\frac{R}{L}\right)^2\frac{\partial}{\partial Z}\left\{\left[\frac{h^3}{12}\,g\beta\,\frac{\partial\Theta}{\partial Z}+\alpha\,\frac{h^5}{80}\left(g\beta\,\frac{\partial\Theta}{\partial Z}\right)^3\right]\right\}=\frac{1}{2}\,\mu R\,u_s\,\frac{\partial(\Theta\,h)}{\partial\theta} \tag{1}$$

where, Θ : fractional film content, h : film thickness, u_s : shaft speed, μ : lubricant viscosity, α : coefficient of plasticity for Rabinowitsch fluids, β is the bulk modulus and $g(\Theta)$ is the switch function which is defined as follows :

$$\begin{cases} g=1 & \text{if} \quad \Theta\geq 1 \\ g=0 & \text{if} \quad \Theta<1 \end{cases} \tag{2}$$

After solving equation (1) for Θ, the pressure distribution can be determined using the following relation [26] :

$$p = p_c + \beta g \ln(\Theta) \tag{3}$$

where, p_c is the cavitation pressure.

2.2 Film thickness relation

The normalized lubricating film geometry for a textured journal bearing takes the following form :

$$h_{(\theta,z)} = h_{smooth\,(\theta)} + \Delta h_{(\theta,z)} \tag{4}$$

where, $h_{smooth\,(\theta)}$ represents the smooth part of the film thickness ($h_{smooth\,(\theta)} = C\ (1 + \varepsilon \cos(\theta - \phi))$) [27] and $\Delta h_{(\theta,z)}$ characterizes the fluid film's depth in the dimple (figure 1) [28].

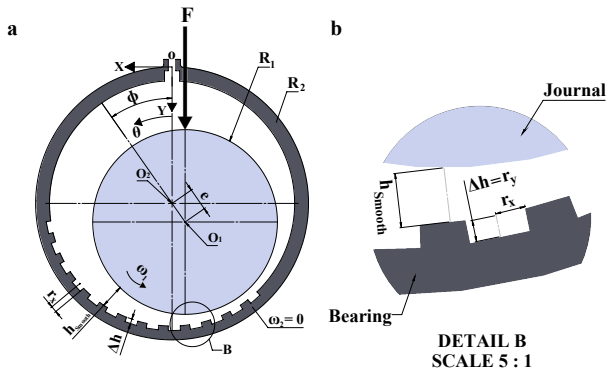

Figure 1: Representative scheme of textured journal bearing

2.3 Optimum textures location

The optimum (partial) surface texturing that improve the bearing performances by increasing the load carrying capacity and so decrease the friction coefficient, have already highlighted in our paper [25], based on Particle Swarm Optimization algorithm (PSO). Table 1 shows the obtained optimum textured area and those imposed in the case of fully textured surface (for comparison point of view).

Table 1: Dimples locations and numbers for fully/optimum textured area [25]

	Fully surface texturing				Optimum surface texturing			
position	θ_1	θ_2	z_1	z_2	θ_1	θ_2	z_1	z_2
	10	350	0	L	42.91°	201.70°	0.05 L	0.98 L
number	nC_θ		nC_z		nC_θ		nC_z	
	12		4		6		4	

2.4 Numerical resolution procedure

The nonlinear mass conservative Rabinowitsch-Reynolds equation (equation 1) has been discretized and solved using the finite differences method with Gauss-Seidel iterative technique. The approaches proposed by Vijayaraghavan and Keith [29], to compute the fractional film content (Θ), and by Fesanghary and Khonsari [30], to improve the convergence speed and avoid the problem in stabilizing the cavitation zone, are employed herein.

- The numerical solution is carried out as per the following steps :

1. Introduction of input data: geometrical parameters, operating conditions, texturing parameters and grid size and convergence criteria ;
2. Compute the film thickness using equation (4) ;
3. Solve the modified Reynolds equation (1) ;
4. Imposition of boundary conditions on affected nodes (JFO condition);
5. The fractional film content is obtained by verifying the following convergence condition: $\dfrac{|\Delta\Theta_{i,j}|}{\Theta_{i,j}} \leq tol_{\Theta}$ at each node (i, j) of the bearing surface mesh ;
6. Once the convergence condition is satisfied, the pressure profile can be determined using equation (3) and then the load attitude angle is calculated ;
7. The computed attitude angle ϕ^k is compared with it's previous value ϕ^{k-1} ;
8. The process stopping after the load attitude angle convergence condition $|\phi^i - \phi^{i-1}| \leq tol_{\phi}$ is satisfied and then the bearing characteristics can be deduced.

2.5 Miscellaneous relations

The load components in the circumferential and the axial direction are given as :

$$\begin{cases} W_\theta = & -\displaystyle\int_0^L \int_0^{2\pi} R\, p\, \cos(\theta - \phi)\, d\theta\, dz \\ W_z = & \displaystyle\int_0^L \int_0^{2\pi} R\, p\, \sin(\theta - \phi)\, d\theta\, dz \end{cases} \tag{5}$$

then, the total bearing load capacity and the attitude angle are :

$$W_c = \sqrt{W_\theta^2 + W_z^2} \tag{6}$$

$$\phi = \arctan\left(\frac{W_\theta}{W_Z}\right) \tag{7}$$

The friction force acting on the shaft surface is calculated by :

$$F_t = \int_0^L \int_0^{2\pi} R^2\, \tau_{\theta,y|y=h}\, d\theta\, dz = \int_0^L \int_0^{2\pi} R^2 \left(\frac{1}{2}\frac{\partial p}{\partial \theta} h + u_s \mu \left(\frac{1}{h} + \frac{h_{\theta_s}}{h^2}\right)\right) d\theta\, dz \tag{8}$$

where, $\tau_{\theta,y}$ is the shear stress in the lubricant film, θ_s is the angular coordinate at the starting cavitation zone and h_{θ_s} is the equivalent of oil film thickness in cavitation zone.

Consequently, the frictional coefficient is obtained as follows :

$$f = \frac{F_{t_s}}{W_c} \tag{9}$$

3 Results and discussion

3.1 Preliminary validation

In the present study, a computer program was developed to investigate the static performances of hydrodynamic finite textured journal bearing, using pseudo-plastic lubricants which obeys to Rabinowitsch fluid model. To establish the validity of the developed computational model, a comparison is performed between our results and those of Tala-Ighil et al. [28] and Wada and Hayashi [8, 9].

For textured journal bearings lubricated with Newtonian fluid, the comparison results are presented in table 2. A good agreement between the two predictions with a slight difference can be observed.

Table 2: Comparison of performance characteristics of textured journal bearings

		Present study		Tala et al. [28]	
Texture cases		Fully	Partially	Fully	Partially
Eccentricity ratio	ε	0.6995	0.5992	0.709	0.595
Minimum film thickness	$h_{min}\,(\mu m)$	9.0145	12.0245	8.71	12.16
Maximum pressure	$P_{max}\,(MPa)$	8.191	7.591	8.26	7.58
Attitude angle	ϕ^o	46.151	49.05	46.1	49.3
Axial flow	Q x 10^{-5} (m^3/s)	1.412	1.714	1.422	1.733

We draw the reader's attention that the details of the previously discussed validation is reported in our works [25, 31, 32].

Thereafter, for smooth journal bearing lubricated with non-Newtonian pseudo-plastic fluid, figure 2 shows the comparison between the present obtained results and those predicted by Wada and Hayashi [8]. It can be noted that the obtained values are very close to the reference ones with a slight difference which probably due to the computational errors in the simulation.

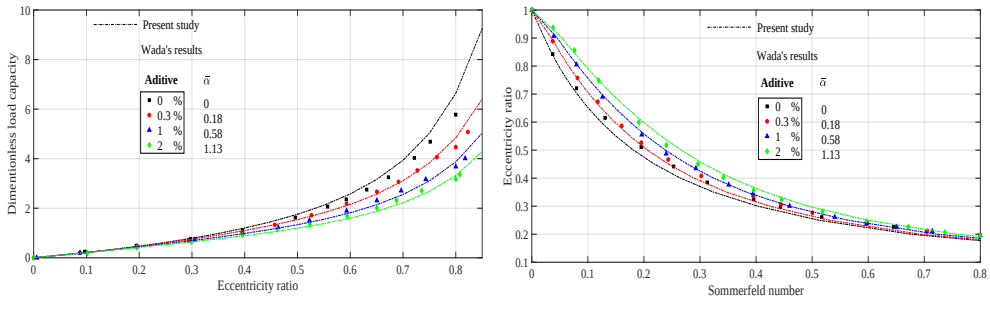

(a) (b)

Figure 2: Comparison present study with Wada's experiments [8]

3.2 Textured journal bearings lubricated with Rabinowitsch fluid model

Here, our purpose is to highlight the influence of non-Newtonian rheology of pseudo-plastic Rabinowitsch fluid on textured journal bearings. To the end, a series of results for smooth/textured bearings lubricated with Newtonian/non-Newtonian fluids are presented and discussed. The bearing geometrical characteristics, operating conditions as well as texturing and computational parameters for studied journal bearing are the same as those used in our study [25].

The two-dimensional 2D comparison between bearing dimensionless pressure profile for Newtonian ($\overline{\alpha} = 0$) and non-Newtonian pseudo-plastic Rabinowitsch fluids ($\overline{\alpha} = 1.2$) cases, and for smooth, fully and optimum textured regions is visualized in figure 3. The pressure profile is plotted in circumferential (at the mid-plane 3a) and axial (at the maximum pressure plane $\theta^o_{p_{max}}$ 3b) directions. It can be observed from this figure that the curves of pseudo-plastic Rabinowitsch pressure profile for all studied cases are less than the Newtonian fluid. This can be explained by the shear-thinning effect (pseudo-plasticity) of the lubricant, in which the fractional film content is reduced, and so decreases the total pressure [8]. Compared to smooth bearing surface, fully texturing with cylindrical texture shape decreases the fractional film content and so the pressure distribution as a results to micro-step bearing mechanism of flat bottom profile [25]. This mechanism produced a large film thickness divergence, which causes a significant pressure drop (in divergent full film region. i.e. between $\theta^o_{p_{max}}$ and $\theta^o_{r\,max}$) and generated a smaller pressure recovery (in cavitation film region), which justified the increases of maximum rupture angle. While, in optimum textured cases a significant improvement in pressure profile is clearly noticed. This behavior can be explained by the effect micro-pressure recovery mechanism [25], where a highest pressure generation is achieved in convergent full film region (i.e. between ϕ^o and $\theta^o_{p_{max}}$).

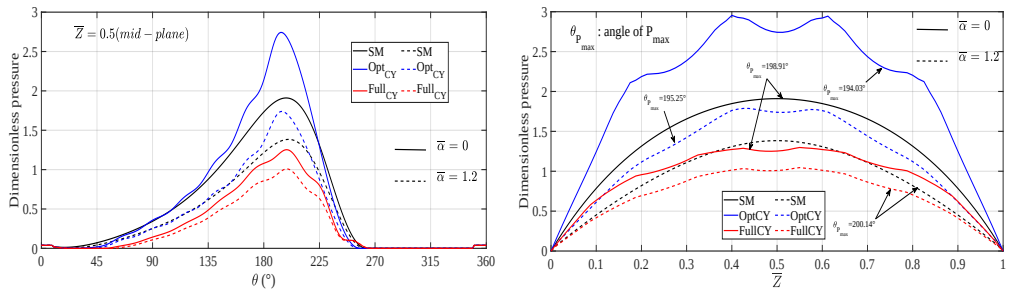

(a) (b)

Figure 3: Comparison between bearing pressure profile for Newtonian/non-Newtonian and smooth/textured cases

Bearing performances as a function of the dimensionless Rabinowitsch pseudo-plasticity coefficient are illustrated in figure 4. The three cases of smooth, fully and optimum texture distributions are investigated with consideration of fixed eccentricity ratio ($\varepsilon = 0.5$) and varying pseudo-plasticity coefficient from 0 to 1.2. From the load carrying capacity curves (figure 4a), it can be discerned for the three cases (smooth/textured), that the load carrying capacity decreases with the increase in pseudo-plasticity coefficient. This behavior is due to the shear-thinning effect (pseudo-plasticity) of the lubricant, in which the total pressure

is reduced. The same observations are reported in [8, 9, 17]. Using fully textured bearing reduces also the load capacity as a results of micro-pressure drop effect, whereas the optimum texturing increases the load lifting capacity due to the dimple pressure recovery generated by textures in the convergent full film region ([25]).

Figure 4b presents the variation of friction coefficient against the Rabinowitsch pseudo-plasticity coefficient. Compared to the load carrying capacity (figure 4a), the variation of resulting friction coefficients values (figure 4b) have an opposite trend. It can be seen that for all studied cases, the friction coefficient increases with the increases of Rabinowitsch pseudo-plasticity coefficient. The reason for this behavior is due to the load capacity of the Rabinowitsch pseudo-plasticity fluids decreasing more than the corresponding decrease of friction force, which cause an increase in friction coefficient. In addition, compared to the smooth surface case, the main feature of fully texturing bearing surfaces is to increase the friction coefficient, as a results of micro-pressure drop effect, which decreases the load carrying capacity, and so increases the friction values. While, the optimum texturing gradually reduced the friction coefficient values, as a results of the increasing load lifting capacity and decreasing friction force, caused by the micro-pressure recovery mechanism ([25]).

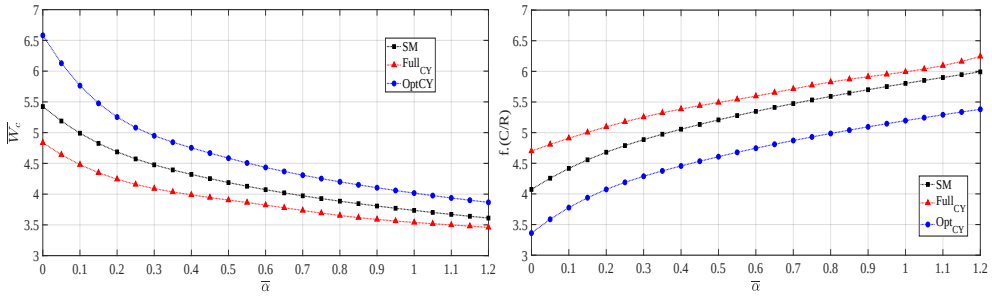

(a) Load carrying capacity

(b) Friction coefficient

Figure 4: Bearing performances against the Rabinowitsch pseudo-plasticity coefficient

4 Conclusion

The present work is dedicated to the effect of pseudo-plastic Rabinowitsch lubricants on the static characteristics of hydrodynamic textured finite groove journal bearings. The obtained results showed that :

1. In case of smooth bearing surface case, the pseudo-plastic Rabinowitsch lubricant decreases the load carrying capacity and increases the friction coefficient as compared to Newtonian fluid, especially at high values of pseudo-plasticity coefficient.

2. In comparison with the smooth case, fully textured bearings with cylindrical dimples have a negative effect on the main bearing performances. While, optimum textured bearings significantly improve all bearing performances.

3. Shear thinning of Rabinowitsch pseudo-plastic lubricants in general reduces the performance of the bearings, and this decrease is more pronounced in fully textured surfaces. While, in the case of optimum textures location a greatest enhancement was obtained, especially at high eccentricity ratios and low pseudo-plasticity effect.

References

[1] M.M. Khonsari, E.R. Booser, *Applied tribology: bearing design and lubrication* (John Wiley & Sons, 2017)

[2] R. Mufti, M. Priest, Proceedings of the Institution of Mechanical Engineers, Part J: Journal of Engineering Tribology **223**, 629 (2009)

[3] A.C. Eringen, International Journal of Engineering Science **2**, 205 (1964)

[4] P. Khatak, H. Garg, Proceedings of the Institution of Mechanical Engineers, Part J: Journal of Engineering Tribology **226**, 775 (2012)

[5] A.C. Eringen, Journal of Mathematics and Mechanics pp. 1–18 (1966)

[6] J.R. Lin, Tribology International **31**, 201 (1998)

[7] S. Tayal, R. Sinhasan, D. Singh, Wear **71**, 15 (1981)

[8] S. Wada, H. Hayashi, Bulletin of JSME **14**, 268 (1971)

[9] S. Wada, H. HAYAsHI, Bulletin of JSME **14**, 279 (1971)

[10] J.R. Lin, L.M. Chu, T.C. Hung, P.Y. Wang, Applied Mathematical Modelling **40**, 8832 (2016)

[11] N.B. Naduvinamani, R. Mareppa, Tribology Online **8**, 242 (2013)

[12] J.R. Lin, Tribology Letters **10**, 237 (2001)

[13] U.P. Singh, Archive of Mechanical Engineering **60**, 247 (2013)

[14] H. Hashimoto, S. Wada (1986)

[15] Y. Hsu (1967)

[16] R. Tanner, Aust. J. Appl. Sci **14**, 29 (1963)

[17] J. JAVOROVA, A. RADULESCU, R. LOVCHALIEVA, N. NIKOLOV, P. KOSTOVA, Tribological Journal BULTRIB p. 248 (2012)

[18] A. Walicka, E. Walicki, P. Jurczak, J. Falicki, International Journal of Applied Mechanics and Engineering **22**, 427 (2017)

[19] S.C. Sharma, A. Singh, Tribology Transactions pp. 1–22 (2020)

[20] P.S. Rao, A. Kumar Rahul, Proceedings of the Institution of Mechanical Engineers, Part C: Journal of Mechanical Engineering Science **233**, 2538 (2019)

[21] F. Rahmani, R. Pandey, J. Dutt, Procedia Technology **23**, 28 (2016)

[22] J. Javorova, A. Mazdrakova, I. Andonov, A. Radulescu, Tribology in Industry **38** (2016)

[23] S. Soni, Proceedings of the Institution of Mechanical Engineers, Part J: Journal of Engineering Tribology p. 1350650121993355 (2021)

[24] S. Kango, R. Sharma, R. Pandey, Tribology International **69**, 19 (2014)

[25] B. Manser, I. Belaidi, S. Khelladi, M.A.A. Chikh, M. Deligant, F. Bakir, Proceedings of the Institution of Mechanical Engineers, Part J: Journal of Engineering Tribology **234**, 1310 (2020)

[26] H. Elrod, Cavitation and related phenomena in lubrication **37** (1974)

[27] B. Vincent, P. Maspeyrot, J. Frêne, in *Tribology Series* (Elsevier, 1995), Vol. 30, pp. 455–464

[28] N. Tala-Ighil, M. Fillon, P. Maspeyrot, Tribology International **44**, 211 (2011)

[29] D. Vijayaraghavan, T. Keith, Journal of tribology **112**, 44 (1990)

[30] M. Fesanghary, M. Khonsari, Journal of Tribology **133**, 024501 (2011)

[31] B. Manser, I. Belaidi, A. Hamrani, S. Khelladi, F. Bakir, Comptes Rendus Mécanique (2019)

[32] B. Manser, I. Belaidi, A. Hamrani, S. Khelladi, F. Bakir, Tribology-Materials, Surfaces & Interfaces **14**, 33 (2020)